

RESEARCH ON EROSION AND WEAR LAW OF STABILIZER BLADE BASED ON CFD-DPM MODEL

Xiaotian Huang¹, Yan Chen^{1,*}, Junqiang Fan²

¹School of Information and Mathematics, Yangtze University, Jingzhou 434023, China

²Well Testing Company, CNPC Bohai Drilling Engineering Co. Ltd, Langfang 065000, China

Email: 520050@yangtzeu.edu.cn

Abstract - In order to study the erosion and wear laws of solid particles on three different structures of centralizers, erosion and wear simulations were conducted on the three structures of centralizers by changing particle diameter, fluid velocity, and particle mass flow rate parameters by using computational fluid dynamics theory and Analysis Fluent DPM model. The results indicate that the erosion rates of the three types of stabilizers increase with the increase of particle size, flow rate, and mass flow rate. The location of erosion on the spiral blade stabilizer is mainly on the inner side of its blade, while the locations of erosion on the concentric and eccentric blade stabilizers are mainly at the connection between the drilling tool and the stabilizer. Scattered spot shaped erosion areas will also be generated at the top of the blade and the flow channel between the blades. Under the same conditions of particle size, flow rate, and mass flow rate, the erosion rate of the spiral blade stabilizer is greater than that of the other two stabilizers. When the particle diameter is large or the flow rate is high, using an eccentric straight edge stabilizer is safer. When the particle concentration in the fluid is high, using a concentric straight edge stabilizer is safer.

Keywords: Stabilizer; Erosion and wear; Mass flow rate; Erosion rate.

1. Introduction

The drill string stabilizer plays a role in centering the drill string and providing a channel for fluid discharge during downhole fluid transportation. The solid particles contained in the fluid can cause erosion and wear on the drill string stabilizer, resulting in the failure of the stabilizer blade. The structural changes of the stabilizer cause changes in pressure drop and flow rate during the discharge of drilling fluid, leading to changes in wellbore fluid pressure and even safety issues. Therefore, studying the erosion and wear law of solid particles on the drill string stabilizer is an important task for safe drilling. At present, scholars at home and abroad have conducted extensive research on the erosion of solid particles on pipes or flow channel structures. For example, Ananya L. et al. [1-4] used Fluent's Discrete Phase Model (DPM) to simulate and analyze the erosion wear of pipes, calculated the maximum erosion rate of various pipe model sizes, and studied the influence of particle size on pipeline erosion wear. The results showed that the erosion within the range of small particles in 1 μm and 9 μm is very small, and the erosion rate of large particles is larger than that of small particles when the particle size increases to 100 μm to 900 μm . Anubhav R. et al. [5-6] found that the parameter dependence of erosion wear at high solid concentration was different from

that observed at low concentration. Compared with relative velocity, erosion wear is more concentration dependent. Gao M. et al. [7-9] studied the erosion rate of pipeline outer wall under different fluid flow conditions using CFD method. The results showed that the faster the fluid flow rate, the more obvious the particle erosion on the bend, and the flow rate was positively correlated with the erosion rate. Parkash O. et al. [10-13] discussed the effect of solid particle concentration on the erosion and wear rate of curved sections by predicting particle concentration, turbulence intensity, and particle tracking, and analyzing the secondary trend of curved sections. The research results showed that the maximum erosion and wear position is located at the convex part of the cross-section at the outlet of the bent pipe. Li M. et al. [14-16] found that the dent of curved pipe can effectively reduce the maximum corrosion rate of elbow. With the crease of the dent depth, the maximum erosion rate of the elbow is reduced. In the harsh conditions of large particle size and high particle speed, dents can better reduce the erosion wear rate.

Literature research has found that there is currently limited research on the flow field at the blade of the drill string stabilizer. This article draws on the numerical simulation calculation methods and experimental experience from the above literature, and based on the CFD-DPM model, conducts erosion

simulation simulations on three different structures of the stabilizer: spiral blade, concentric straight edge, and eccentric straight edge. The effects of particle diameter, fluid velocity, and particle mass flow rate on the erosion wear of the stabilizer are analyzed, and the relevant conclusions can provide some reference for the optimization design of the stabilizer structure.

2. Theoretical Calculation Model

2.1 Particle Motion Equation

Some Literatures only consider the unidirectional influence of continuous relative discrete phase by using Lagrangian method to track particles and unidirectional coupling method, and ignoring the interaction between particles and the influence of particles relative to fluid phase. By solving the motion equation of particles to track them, and substituting the information of collisions between particles into the erosion equation, the corresponding erosion rate is ultimately determined. The main particle motion equations used are as follows:

$$\frac{dV_p}{dt} = F_D(U - V_p) + \frac{g(\rho_p - \rho)}{\rho_p} + F_{others} \quad (1)$$

Where:

$$F_D = \frac{18\mu C_D Re}{\rho_p d_p^2 \cdot 24} \quad (2)$$

In the formula, F_D is the drag force per unit mass of particles, μ is the dynamic viscosity, U is the fluid velocity, V_p is the particle velocity, ρ_p is the particle density, g is the gravitational acceleration, is the particle size, C_D is the resistance coefficient, F_{others} is the other forces per unit mass, and Re is the relative Reynolds number.

2.2 Turbulence Model

Using RNG k- ϵ turbulence model simulates erosion calculation, which uses turbulent kinetic energy k and turbulent flow energy dissipation rate ϵ of the two equations, and compared with the model of standard k- ϵ , an additional condition has been added to the equation of ϵ of RNG k- ϵ model to more accurately calculate high-speed flow. The equations for turbulent kinetic energy and turbulent dissipation rate are as follows:

$$\begin{aligned} \frac{\partial}{\partial t}(\rho k) + \frac{\partial}{\partial x_i}(\rho k u_i) &= \frac{\partial}{\partial x_j}(\alpha_k u_{eff} \frac{\partial k}{\partial x_j}) + \\ G_k + G_b - \rho \dot{\epsilon} - Y_M + S_k & \end{aligned} \quad (3)$$

$$\frac{\partial}{\partial t}(\rho \epsilon) + \frac{\partial}{\partial x_i}(\rho \epsilon u_i) = \frac{\partial}{\partial x_j}(\alpha_\epsilon u_{eff} \frac{\partial \epsilon}{\partial x_j}) + \quad (4)$$

$$C_{1\epsilon} \frac{\epsilon}{k} (G_k + C_{3\epsilon} G_b) - C_{2\epsilon} \rho \frac{\epsilon^2}{k} - R_\epsilon + S_\epsilon$$

In the formula, $C_{1\epsilon} = 1.42$, $C_{2\epsilon} = 1.68$. μ_i is the velocity of the fluid, μ_{eff} is the dynamic viscosity of the fluid, G_k is the turbulent kinetic energy generated by the average velocity gradient, G_b is the turbulent kinetic energy generated by buoyancy, Y_M is the contribution of turbulent wave expansion in compressible turbulence to the total dissipation rate, S_k and S_ϵ are user-defined source terms.

2.3 Discrete Phase Control Equation

The CFD-DPM model is applied for particle erosion calculation, and the Lagrange equation is used to track the particles. Newton's second law of motion is used as the discrete phase control equation. The mechanical equilibrium equation of the particles is expressed as follows:

$$m_p \frac{du_p}{dt} = F_D + F_G + F_P \quad (5)$$

Where:

$$F_D = m_p \frac{u - u_p}{\tau_r} \quad (6)$$

$$F_G = m_p g \frac{\rho_p - \rho}{\rho_p} \quad (7)$$

$$F_P = m_p \frac{\rho}{\rho_p} \frac{r}{u} \nabla u \quad (8)$$

In the formula, m_p is the mass of particles, u_p is the velocity of particles, F_D is the resistance, F_G is the sum of gravity and buoyancy, F_P is the pressure gradient force, and τ_r is the relaxation time of particles are defined as:

$$\tau_r = \frac{4\rho_p d_p^2}{3\mu C_d Re_p} \quad (9)$$

The particle resistance coefficient C_d is defined as:

$$C_d = a_1 + \frac{a_2}{Re_p} + \frac{a_3}{Re_p^2} \quad (10)$$

Among them, a_1, a_2 , and a_3 are constants, and are particle Reynolds numbers, given by the following equation:

$$Re_p = \frac{\rho d_p |u_p - u|}{\mu} \quad (11)$$

In the DPM model, due to the very sparse particle concentration, the interaction between particles and the influence of particle volume fraction on fluid flow can be ignored, and the rotation of particles during fluid flow is not considered. The erosion wear formula is:

$$R_{erosion} = \sum_{n=1}^N \frac{m_k C(d_k) f(\alpha) u_k^{b(v)}}{A_{face}} \quad (12)$$

In the formula, $R_{erosion}$ is the erosion and wear rate of the wall surface, N is the number of collision particles, m_k is the particle mass flow rate, and $C(d_k)$ is a function of particle diameter. After consulting data, $C(d_k) = 1.8 \times 10^{-9}$, and it is found that u_k is the velocity of particles relative to the wall surface, $b(v)$ is a function of relative velocity, takes 2.6, A_{face} is the area of the wall calculation unit, $f(\alpha)$ is the impact angle function, and is defined using segmented interpolation method, as shown in Table 1:

Table 1 Impact angle function values

Impact angle/(°)	0	20	30	45	90
Function value	0	0.8	1	0.5	0.4

In erosion simulation, the wall recovery coefficient is used to represent the motion behavior of particles rebounding after colliding with the wall. The commonly used wall recovery coefficient models currently include the collision model proposed by Forde and the collision model proposed by Grant and Tabakoff. The latter is used in this article for description, and its expression is:

$$\begin{aligned} e_n &= 0.993 - 1.76\alpha + 1.56\alpha^2 - 0.49\alpha^3 \\ e_t &= 0.988 - 1.66\alpha + 2.11\alpha^2 - 0.67\alpha^3 \end{aligned} \quad (13)$$

Among them, e_n is the normal recovery coefficient, e_t is the tangential recovery coefficient, α is the impact angle, and the unit is rad.

3. Flow Field Model and Grid Division

3.1 Flow Field Model

Fig. 1 shows the flow field models of three different structures of centralizers: spiral blade, concentric straight edge, and eccentric straight edge. The model involves connecting a section of drilling tool at each end of the centralizer and placing it inside the wellbore. The annular area between the inner wall of the wellbore and the outer wall of the centralizer is extracted as the fluid domain. The inner diameter of the drilling tool, the inner diameter of the wellbore, and the length of the entire fluid domain is set to ensure sufficient fluid flow.

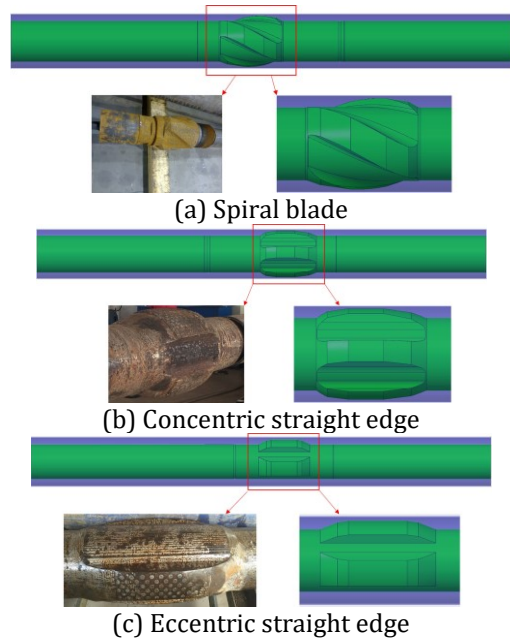


Figure 1: Flow field structure models of centralizers

In order to ensure the quality of grid division, ANSYS SpaceClaim software is used to simplify the geometry of the flow field model before grid division. Small details such as small radius fillets and small step surfaces that do not affect the structural characteristics of the model are removed. Due to the complex geometric features of the stabilizer, unstructured mesh partitioning is adopted, and a tetrahedral mesh is used as a whole. Fig.2 shows the grid partitioning of flow field models for three types of structural stabilizers.

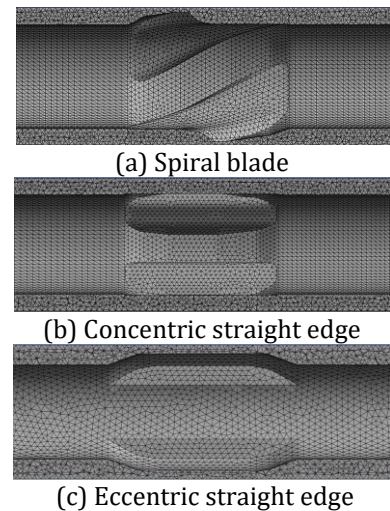


Figure 2: Three types of centralizer grid models

3.2 Boundary Condition

The fluid phase inside the fluid domain is drilling fluid, with a density of 1080kg/m³ and a viscosity of 0.012Pa·s. The inlet is set as a velocity inlet, the inlet flow rate is 5m/s, and the outlet is set as free flow. The discrete phase particles are sand particles, using

a DPM model with a density of 2550kg/m³. The injection source type is surface incidence, with the same incidence velocity as the fluid flow rate and a mass flow rate of 1.1kg/s. The discrete random trajectory model is enabled. The calculation method adopts SIMPLE method, and the turbulent kinetic energy and turbulent dissipation rate adopt second-order upwind scheme.

4. Simulation Results and Analysis

4.1 Analysis of Flow Field Characteristics

In order to study the flow characteristics of the flow field in the stabilizer section, velocity trajectory Contours of the cross-section of the flow field at the spiral blade, concentric straight edge, eccentric straight edge blade, or straight edge were taken separately, as shown in Fig.3. The flow fields of the three structures have a common feature at this position, that is, a swirling velocity vortex will appear at the boundary of the blade or straight edge. This is because the fluid encounters a sudden change position during the flow process, and a velocity vortex will form behind the sudden change position, indicating that at this position, the particles will collide with the wall at that position when solid particles are carried in the fluid, causing erosion and wear on the blade or straight edge.

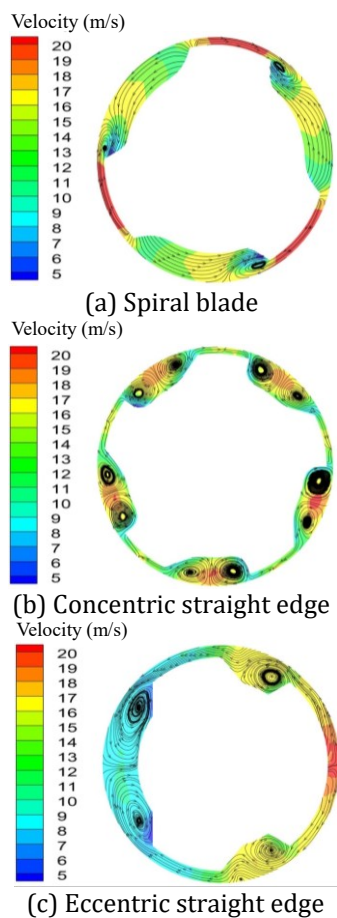


Figure 3: Velocity traces diagrams of three types of stabilizers

Fig. 4 is the velocity vector diagrams of the flow field of three types of stabilizers. Fig. 4 shows that at the blade or straight edge, the fluid velocity reaches its maximum value. Therefore, at this position, the solid particles carried in the fluid collide more severely with the wall, resulting in greater erosion and wear.

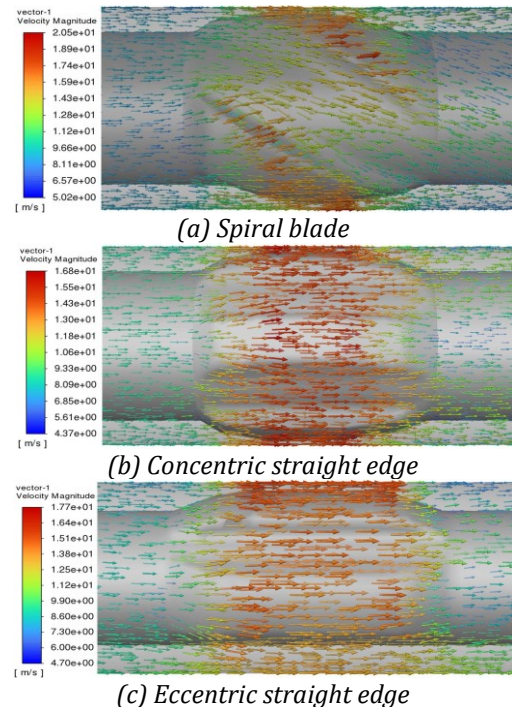


Figure 4: Velocity vector diagrams of three types of stabilizers

4.2 Erosion Simulation Analysis

Studying the erosion and wear laws of solid particles on three types of structure stabilizers, namely spiral blade, concentric straight edge, and eccentric straight edge, is of great significance for the structural optimization and safety evaluation of stabilizers. This article adopts the analysis method of controlling variables to analyze the impact of changes in particle diameter, fluid velocity, and particle mass flow rate on the maximum erosion rate of the stabilizer.

4.2.1 The Influence of Particle Diameter on Erosion Rate

Under the conditions of a fluid flow rate of 5m/s and a particle mass flow rate of 1.1kg/s, analyze the impact of different particle sizes on the erosion wear of the stabilizer. As shown in Fig.5-Fig.7, erosion and wear Contours were extracted for four different particle sizes: 0.2mm, 0.4mm, 0.6mm, and 0.8mm.

Fig. 5 shows that the area of erosion and wear on the spiral blade stabilizer is mainly distributed in a strip shape on the inner side of the blade, as well as at the connection between the drilling tool and the stabilizer. As the particle size increases, the area of erosion and wear on the inner side of the blade does

not change significantly. However, the area of erosion and wear will gradually increase at the connection between the drilling tool and the stabilizer.

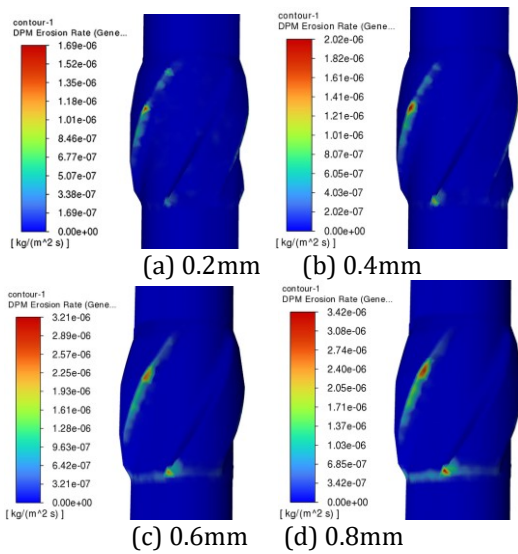


Figure 5: Contour of erosion and wear of spiral blade under different particle sizes

Fig. 6 shows the area where the concentric straight edge stabilizer is subjected to erosion and wear is mainly at the connection between the drilling tool and the stabilizer. A spotted erosion area will be formed at the flow channel between the straight edges when the particle size is less than 0.4mm. It shows the smaller the particle size at the same mass flow rate, the more particles carried by the fluid per unit volume, causing some particles to deposit in the flow channel and cause erosion and wear on the flow channel wall. As the particle size increases, the pitting area at the flow channel gradually decreases and eventually disappears.

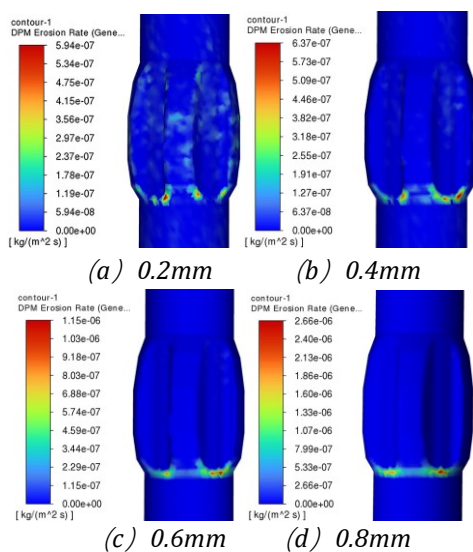


Figure 6: Contour of erosion and wear of concentric straight edges under different particle sizes

Fig. 7 shows that the eccentric straight edge stabilizer will produce a spotted erosion area at the flow channel between the top of the straight edge and the straight edge when the particle size is less than 0.4mm. The pitting erosion area at the top of the straight edge and the flow channel disappears when the particle size increases to above 0.4mm. However, it will cause erosion and wear at the connection between the drilling tool and the stabilizer, and as the particle size increases, the area of erosion and wear at the connection between the drilling tool and the stabilizer will significantly increase.

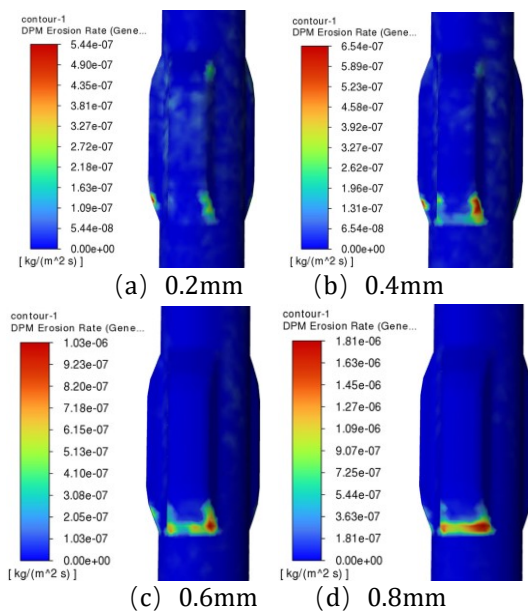


Figure 7: Contour of erosion and wear of eccentric straight edges under different particle sizes

Fig. 8 is the erosion rate variation curves of three types of structural stabilizers under different particle sizes. It can be seen that as the particle size increases, the erosion rates of all three types of stabilizers also increase. Its mass also increases accordingly as the particle size increases. According to the definition of momentum, under a constant flow rate, the momentum generated also increases when the mass of the particles increases, thereby intensifying the impact on the wall of the stabilizer. Therefore, the amount of erosion and wear caused by the wall also increases. Through comparison, it was found that the erosion rate of the spiral blade stabilizer was the highest under the same particle size, and the erosion rate of the eccentric straight edge stabilizer was the lowest. Therefore, when there are large particles in the fluid, it is advisable to choose an eccentric straight edge structure stabilizer.

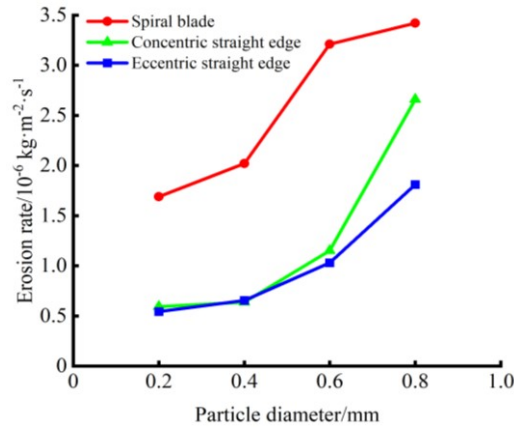


Figure 8: Erosion and wear patterns of centralizers with different particle sizes

4.2.2 The Influence of Fluid Velocity on Erosion Rate

Changing the fluid flow rate is used to analyze the impact of different flow rates on the erosion wear of the stabilizer under the condition of a particle diameter of 0.2mm and a particle mass flow rate of 1.1kg/s. As shown in Fig.9-Fig.11, extract erosion and wear Contours for four different flow rates of 5m/s, 7m/s, 9m/s, and 11m/s, respectively.

Fig. 9 shows that the area of erosion and wear on the spiral blade stabilizer is still distributed in a strip shape on the inner side of the blade, and with the increase of flow velocity, the size of the area of erosion and wear on the inner side of the blade does not change significantly. Due to the shorter distance between the erosion wall and the stabilizer and the flow velocity of the fluid increases, the time for particles to impact the wall is less, so that the erosion area on the wall does not change significantly with the increase of flow velocity.

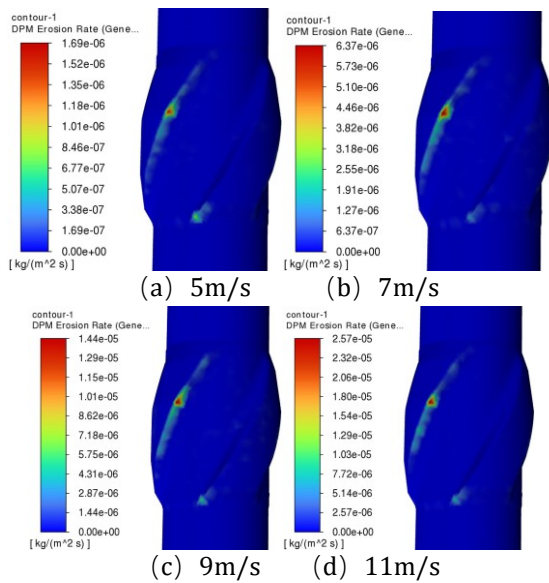


Figure 9: Contour of erosion and wear of spiral blade under different flow velocities

Fig. 10 shows that the area where the concentric straight edge stabilizer is subjected to erosion and wear is mainly at the connection between the drilling tool and the stabilizer. Due to the small particle diameter, particles carried by the fluid will enter the flow channel between the straight edges and collide with the wall surface, causing erosion and wear, forming a spotted erosion area at the flow channel. As the flow rate increases, the particles carried by the fluid leave the channel area faster, causing the pitting area at the channel to gradually decrease.

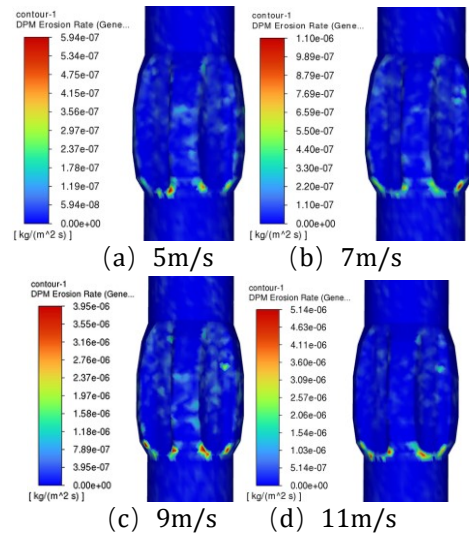


Figure 10: Contour of erosion and wear of concentric straight edges under different flow velocities

Fig. 11 shows the area where the eccentric straight edge stabilizer is subjected to erosion and wear is mainly at the connection between the drilling tool and the stabilizer. A spotted erosion area will be generated at the flow channel between the straight edges when the flow rate is less than 7m/s. As the flow rate increases, the pitting area at the flow channel disappears, and the area of erosion and wear at the connection between the drilling tool and the stabilizer will significantly increase.

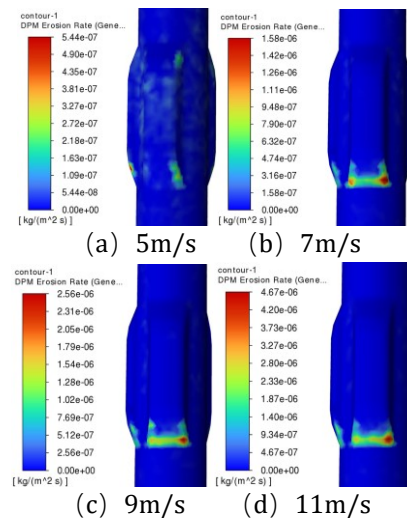


Figure 11: Contour of erosion and wear of eccentric straight edges under different flow velocities

Fig. 12 is the erosion rate variation curves of three types of stabilizers under different flow velocities. As the flow velocity increases, the erosion rates of all three types of stabilizers also increase. This is because as the fluid velocity increases, the velocity of particles carried in the fluid also increases accordingly. According to the definition of kinetic energy, when the particle mass is constant, the kinetic energy generated by the particle also increases as its velocity increases. The degree of impact on the wall of the stabilizer will be greater, resulting in greater erosion and wear on the wall. Through comparison, it was found that at the same flow rate, the erosion rate of the spiral blade stabilizer was the highest. When the flow rate was greater than 7m/s, the erosion rate of the concentric straight edge stabilizer was greater than that of the eccentric straight edge stabilizer. Therefore, when the fluid flow rate is high, it is advisable to choose a stabilizer with an eccentric straight edge structure.

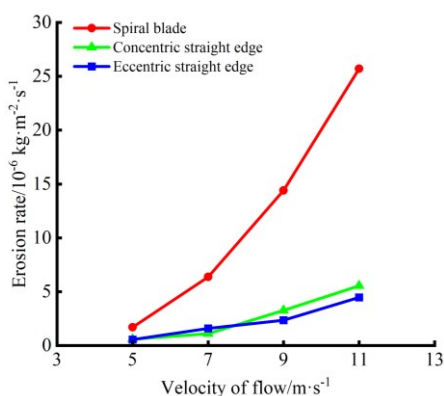


Figure 12: Erosion and wear patterns of centralizers under different flow velocities

4.2.3 The Influence of Particle Mass Flow Rate on Erosion Rate

Under the condition of a particle diameter of 0.2mm and a fluid velocity of 5m/s, changing the mass flow rate of the particles is used to analyze the impact of different mass flow rates on the erosion wear of the stabilizer. As shown in Fig.13-Fig.15, erosion and wear Contours were extracted for four different mass flow rates: 0.8kg/s, 1.0kg/s, 1.2kg/s, and 1.4kg/s.

Fig.13 shows that the area of erosion and wear on the spiral blade stabilizer is mainly distributed in a strip shape on the inner side of the blade, and the size of the area of erosion and wear on the inner side of the blade does not change significantly with the increase of mass flow rate. This is because the flow velocity of the fluid is relatively high, and the distance between the eroded walls is short, so the area affected by erosion and wear will not undergo significant changes with the increase of mass flow rate.

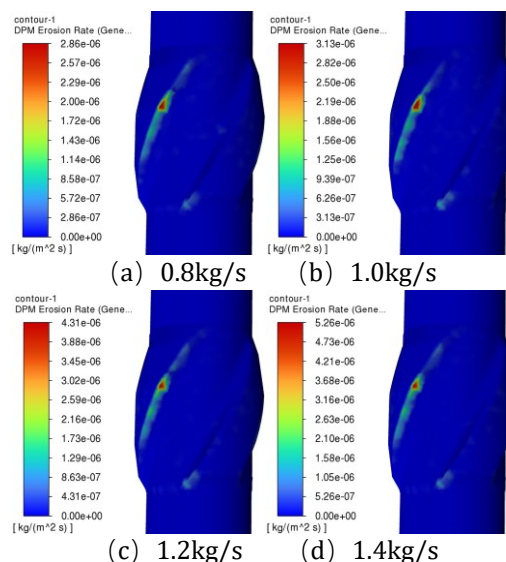


Figure 13: Contour of erosion and wear of spiral blade under different mass flow rates

Fig. 14 shows that the area where the concentric straight edge stabilizer is subjected to erosion and wear is mainly at the connection between the drilling tool and the stabilizer, and there will also be a spotted erosion area in the flow channel between the straight edges. With the increase of mass flow rate, there is no significant change in the erosion and wear area mentioned above. This is because when the particle size is small, the mass will also be smaller, resulting in weaker inertial forces on particles mixed in the fluid, which has limited impact on wall erosion and wear. Therefore, the area affected by erosion and wear will not change significantly with the increase of mass flow rate.

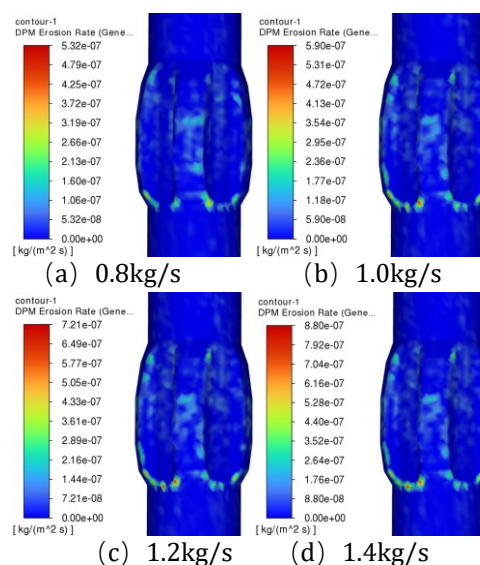


Figure 14: Contour of erosion and wear of concentric straight edges under different mass flow rates

Fig. 15 shows that the area where the eccentric straight edge stabilizer is subjected to erosion and wear is mainly at the connection between the drilling tool and the stabilizer. Due to the small particle size, the particles are carried by the fluid into the flow channel between the straight edges, which will also cause erosion and wear on the flow channel. As the mass flow rate increases, there is no significant change in the areas subject to erosion and wear mentioned above.

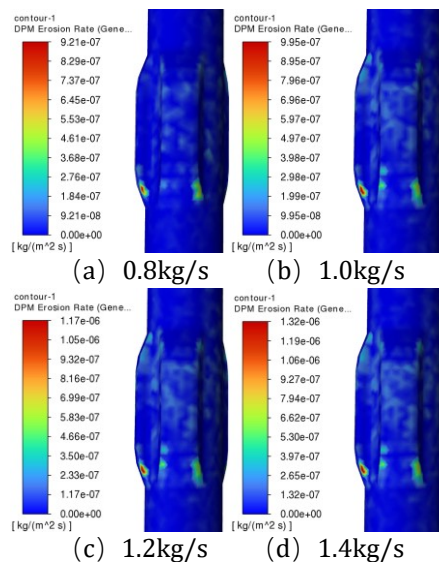


Figure 15: Contour of erosion and wear of eccentric straight edges under different mass flow rates

Fig. 16 is the erosion rate variation curves of three types of stabilizers under different mass flow rates. It can be seen that as the mass flow rate increases, the erosion rates of all three types of stabilizers also increase. This is because, under a constant particle size, as the mass flow rate increases, the number of particles carried in the fluid per unit volume will also correspondingly increase, leading to more particles colliding and impacting the wall, resulting in greater erosion and wear on the wall. Through comparison, it was found that under the same mass flow rate, the erosion rate of the spiral blade stabilizer was the highest, while the erosion rate of the concentric straight edge stabilizer was the lowest. Therefore, when the particle concentration in the fluid is high, it is advisable to choose a centralizer with a concentric straight edge structure.

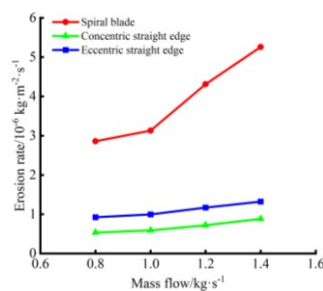


Figure 16: Erosion and wear patterns of centralizers under different mass flow rates

5. Conclusions

Through erosion simulation analysis of three types of structural stabilizers, the following conclusions are drawn:

(1) The location of erosion on the spiral blade stabilizer is mainly on the inner side of its blade, while the locations of erosion on the concentric and eccentric blade stabilizers are mainly at the connection between the drilling tool and the stabilizer. There will also be scattered spotted erosion areas at the top of the blade and the flow channel between the blades.

(2) With the change of fluid parameters, the erosion area of the spiral blade stabilizer does not change significantly. The particle size has a more significant impact on the erosion of the concentric straight edge stabilizer. As the particle size gradually increases, the pitting area at the flow channel between the straight edges of the concentric straight edge stabilizer will gradually decrease and eventually disappear.

(3) The factors that have a more significant impact on the eccentric straight edge stabilizer due to erosion are particle size and flow velocity. As the particle size and flow velocity gradually increase, the pitting area at the flow channel between the eccentric straight edges of the stabilizer will disappear, and the area of erosion and wear at the connection between the drilling tool and the stabilizer will significantly increase.

(4) Although the erosion rates of the three types of stabilizers all show a corresponding increasing trend with the increase of particle size, flow rate, and particle mass flow rate, under the same conditions of particle size, flow rate, and mass flow rate, the erosion rate of the spiral blade stabilizer is significantly higher than that of the other two types of stabilizers. The eccentric straight edge stabilizer is safer when the particle diameter is large or the flow velocity is high. It is safer to use a concentric straight edge stabilizer when the particle concentration in the fluid is high.

References

- [1] Ananya Latchupatula, Kumar Baghel Yatish, Kumar Patel Vivek. Computational Analysis of Erosion Wear in Various Angle Bent Pipes[J]. Materials Today: Proceedings, Volume 80, Issue 1, Pp: 1150-1157, 2023. doi: <https://doi.org/10.1016/j.matpr.2022.12.123>.
- [2] Du Xiaochao, Liu Shuai, Liu Peng, et al. Numerical Simulation of Pipeline Erosion of Particulate Matter in LBE Based on DPM Model[J]. Nuclear Power Engineering, Volume 42, Issue 2, Pp: 48-

- 53, 2021. doi: <https://doi.org/10.13832/j.jnpe.2021.01.0048>.
- [3] GUAN W, Jianfei D, Linyuan K, et al. Study on the influence of structural parameters on the flow and cavitation characteristics of tandem multi-stage pressure-reducing valves[J]. *Flow Measurement and Instrumentation*, Volume 87, Pp: 102230, 2022. <https://doi.org/10.1016/j.flowmeasinst.2022.102230>.
- [4] Wang H, Zhu Z, Zhang M, et al. Investigation on cavitating flow and parameter effects in a control valve with a perforated cage[J]. *Nuclear Engineering and Technology*, Volume 53, Issue 8, Pp: 2669-2681, 2021. doi: <https://doi.org/10.1016/j.net.2021.02.003>.
- [5] Anubhav Rawat, S.N. Singhn, V. Seshadri. Erosion wear studies on high concentration fly ash slurries[J]. *Wear*, Volume 378-379, Pp:114-125, 2017. doi: <http://dx.doi.org/10.1016/j.wear.2017.02.039>.
- [6] Enbo Zhang, Dezhi Zeng, Hongjun Zhu, et al. Numerical simulation for erosion effects of three-phase flow containing sulfur particles on elbows in high sour gas fields [J]. *Petroleum*, Issue 4, Pp: 1160-1171, 2018. doi: <https://doi.org/10.1016/j.petlm.2017.12.008>.
- [7] Gao Mingxing, Zhou Yadong, Cao Kai, et al. Erosion Behavior of Non-Newtonian Sand-Carrying Liquid Elbow During Large Displacement Fracturing[J]. *Lecture Notes in Electrical Engineering*, Volume 935, Issue 4, Pp: 1160-1171, 2022. doi: https://doi.org/10.1007/978-981-19-4132-0_159.
- [8] Wang Mengyi, Chen Yan, Liu Yang, et al. Analysis and Optimization of Fluid Solid Coupling Erosion in Gas Pipeline Based on DPM Model [J]. *Journal of Failure Analysis and Prevention*, Volume 23, Issue 4, Pp: 1701-1714, 2023. doi: <https://doi.org/10.1007/s11668-023-01716-6>.
- [9] Liming Yao, Yuxi Liu, Zhongmin Xiao, et al. Investigation on tee junction erosion caused by sand-carrying fracturing fluid [J]. *Tribology International*, Volume 179, Pp: 108157, 2023. doi: <https://doi.org/10.1016/j.triboint.2022.108157>.
- [10] Parkash Om, kumar Arvind, Sikarwar Basant Singh, et al. CFD modeling of slurry flow erosion wear rate through mitre-pipe bend[J]. *Proceedings of the Institution of Mechanical Engineers, Part C: Journal of Mechanical Engineering Science*, Volume 236, Issue 5, Pp: 2256-2267, 2023. doi: <https://doi.org/10.1177/09544062211026353>.
- [11] Baghel Yatish Kumar, Patel Vivek Kumar. Computational investigation of erosion wear in the eco-friendly disposal of the fly ash through 90° horizontal bend of different radius ratios[J]. *Chemical Product and Process Modeling*, Volume 18, Issue 3, Pp: 411-422, 2023. doi: <https://doi.org/10.1515/cppm-2022-0026>.
- [12] Guofu Ou, Kainian Bie, Zhijian Zheng, et al. Numerical simulation on the erosion wear of a multiphase flow pipeline [J]. *Int Journal of Adv Manuf Technol*, Volume 96, Pp: 1705-1713, 2018. doi: <https://doi.org/10.1007/s00170-017-0834-8>.
- [13] Amir Mansourin, Hadi Arabnejad, Soroor Karimi, et al. Improved CFD modeling and validation of erosion damage due to fine sand particles [J]. *Wear*, Volume 338-339, Pp: 339-350, 2015. doi: <http://dx.doi.org/10.1016/j.wear.2015.07.011>.
- [14] Li MO, Zhiyuan WANG, Shulu FENG, et al. Erosion Mechanism and Sensitivity Parameter Analysis of an Innovative Shaped Curved Pipeline [J]. *MECHANIKA*, Volume 26, Issue 6, Pp: 511-517, 2020. doi: <https://doi.org/10.5755/j01.mech.26.6.24767>.
- [15] Bahareh Nemati, Mohammad Vaghefi, Mahdi Behrooz. Numerical investigation of the erosion reduction in elbows using separate and helical inner ring [J]. *Results in Engineering*, Volume 23, Pp: 102499, 2024. doi: <https://doi.org/10.1016/j.rineng.2024.102499>.
- [16] Rehan Khan, Michał Wiczorowski, Asiful H. Seikh, et al. Experimental and numerical study of erosive wear of t-pipes in multiphase flow[J]. *Engineering Science and Technology*, Volume 52, Pp: 101683, 2024. doi: <https://doi.org/10.1016/j.jestch.2024.101683>.